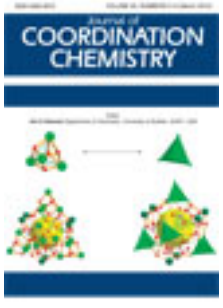

Journal of Coordination Chemistry
Publication details, including instructions for authors and subscription information:
http://www.tandfonline.com/loi/gcoo20

Structural study of picolinamide complexes of Ni(II), Zn(II), Cd(II), and Hg(II) nitrates in solid state and solution

Marijana Đaković [a], Marijana Vinković [b], Sunčica Roca [b], Zora Popović [a], Ivan Vicković [a], Dražen Vikić-Topić [b], Josip Lukač [c], Nikola Đaković [c d] & Zvonko Kusić [c d]

[a] Laboratory of General and Inorganic Chemistry, Department of Chemistry, Faculty of Science, University of Zagreb, Horvatovac 102a, HR-10000 Zagreb, Croatia

[b] NMR Centre, Ruđer Bošković Institute, Bijenička cesta 54, HR-10000 Zagreb, Croatia

[c] Department of Oncology and Nuclear Medicine, University Hospital Center "Sestre Milosrdnice", School of Medicine, University of Zagreb, Vinogradska cesta 29, HR-10000 Zagreb, Croatia

[d] Croatian Academy of Sciences and Arts, Zrinjski trg 11, HR-10000 Zagreb, Croatia

Published online: 01 Mar 2012.

To cite this article: Marijana Đaković, Marijana Vinković, Sunčica Roca, Zora Popović, Ivan Vicković, Dražen Vikić-Topić, Josip Lukač, Nikola Đaković & Zvonko Kusić (2012) Structural study of picolinamide complexes of Ni(II), Zn(II), Cd(II), and Hg(II) nitrates in solid state and solution, Journal of Coordination Chemistry, 65:6, 1017-1032, DOI: 10.1080/00958972.2012.663912

To link to this article: http://dx.doi.org/10.1080/00958972.2012.663912

Journal of Coordination Chemistry
Vol. 65, No. 6, 20 March 2012, 1017–1032

Structural study of picolinamide complexes of Ni(II), Zn(II), Cd(II), and Hg(II) nitrates in solid state and solution

MARIJANA ĐAKOVIĆ*†, MARIJANA VINKOVIĆ*‡, SUNČICA ROCA‡, ZORA POPOVIĆ†, IVAN VICKOVIĆ†, DRAŽEN VIKIĆ-TOPIĆ‡, JOSIP LUKAČ§, NIKOLA ĐAKOVIĆ§¶ and ZVONKO KUSIĆ§¶

†Laboratory of General and Inorganic Chemistry, Department of Chemistry, Faculty of Science, University of Zagreb, Horvatovac 102a, HR-10000 Zagreb, Croatia
‡NMR Centre, Ruđer Bošković Institute, Bijenička cesta 54, HR-10000 Zagreb, Croatia
§Department of Oncology and Nuclear Medicine, University Hospital Center ''Sestre Milosrdnice'', School of Medicine, University of Zagreb, Vinogradska cesta 29, HR-10000 Zagreb, Croatia
¶Croatian Academy of Sciences and Arts, Zrinjski trg 11, HR-10000 Zagreb, Croatia

(*Received 18 November 2011; in final form 19 January 2012*)

Three picolinamide complexes of nickel(II) (**1**), zinc(II) (**2**), and cadmium(II) (**3**) have been prepared and their solid state structures were determined by single-crystal X-ray diffraction analysis. Their structures in DMSO solutions as well as the structure of similar mercury(II) complex, $[Hg(NO_3)(pia)_2](NO_3)$ (**4**), have been elucidated by ^1H and ^{13}C NMR spectra. The picolinamide is bound through the *N*,*O*-donors in all four complexes in solid state, but only in **4** it is in solution state. In nickel (**1**), zinc (**2**), and cadmium (**3**) complexes the pia-*N* coordination in solution is suggested. The X-ray analysis revealed that isomorphous nickel (**1**) and zinc (**2**) crystal structures comprise the centrosymmetrical *trans*-$[M(H_2O)_2(pia)_2]^{2+}$ (M = Ni, Zn; pia = picolinamide) and nitrate. The crystal lattices also contain two non-coordinated H_2O molecules. In **3**, each cadmium(II) is *N*,*O*-chelated by two *cis*-oriented pia ligands, while remaining coordination sites of the capped pentagonal bipyramid are occupied by three oxygen atoms from two nitrates. Crystal structures are dominated by O/N/C–H···O hydrogen bonds. The carboxamide moieties in **1** and **2** do not form any head-to-head or catemeric supramolecular synthons, but participate in the formation of R_4^4 (12) motifs with solely the amide nitrogen atoms as double hydrogen bond donors. In **3**, neighboring molecules are linked into head-to-head amide dimers. The biological effect of picolinamide and $[Zn(pia)_2(H_2O)_2](NO_3)_2$ on ingestion and intracellular microbicidal capacities of human peripheral blood phagocytes was also assessed.

Keywords: Picolinamide complexes; NMR; Crystal structure; Hydrogen bonding; Phagocytosis

1. Introduction

The binding of metal ions by peptides (amides) and proteins is of fundamental interest because of the importance of metal ions in biological systems [1]. Metal could be part of the active site of enzymes, stabilizing the macromolecular structure of the proteins and

*Corresponding authors. Email: mdjakovic@chem.pmf.hr; mvinkovi@irb.hr

ISSN 0095-8972 print/ISSN 1029-0389 online
http://dx.doi.org/10.1080/00958972.2012.663912

affecting enzymes or membranes to control all metabolism [2–4]. The behavior of pyridinecarboxamides towards biologically relevant d-block metals has been widely investigated due to its ability to mimic various active sites of metalloproteins [5].

As part of our ongoing research on heteroleptic pyridinecarboxamide complexes of the 3d-block metals as well as of group 12 in the presence of various ions of different steric and electronic demands (NCS^-, N_3^-, CNO^-, NO_3^-, ClO_4^-, SO_4^{2-}, etc.) [6], we have undertaken investigation on nitrate complexes of Ni(II), Zn(II), Cd(II) with picolinamide. Besides biological activity of picolinamide [7], its metal complexes [8] as well as nitrate [9–12], utilization of multidentate *O*- and/or *N*-donor ligands is an effective strategy in the construction of various types of coordination [13, 14] as well as supramolecular networks [15, 16]. The aim of this work was to further the understanding of the impact of counter-ions on amide hydrogen bonding in assembling metal-containing building blocks, since these influence a compound's solubility and other physical properties.

In this article, we report the synthesis, spectroscopic, and molecular and crystal structure determination of three picolinamide complexes, isostructural $[Ni(pia)_2(H_2O)_2](NO_3)_2$ (**1**) and $[Zn(pia)_2(H_2O)_2](NO_3)_2$ (**2**), as well as $[Cd(pia)_2(NO_3)_2]$ (**3**). With the aid of ^1H and ^{13}C NMR spectra, we characterize the species that are present in DMSO solution of **1**–**3**, and $[Hg(pia)_2(NO_3)](NO_3)$ (**4**) known from our earlier study [6c]. The interplay of coordination sphere around metal center and hydrogen bonding in 3-D supramolecular architecture is also discussed. Furthermore, we report the biological effects on phagocytosis of picolinamide and its zinc complex $[Zn(pia)_2(H_2O)_2](NO_3)_2$ (**2**) because (a) zinc affects multiple aspects of the immune systems [17] and (b) metal complexes are sometimes more biologically effective than uncoordinated ligands [18].

2. Experimental

2.1. *Materials and physical measurements*

All chemicals were purchased from Aldrich Chemical Co. and used as received without purification. CHN-microanalyses were performed in a Perkin-Elmer 2400 Series II CHNS analyzer in the Chemical Analytical Service Laboratories of the Ruđer Bošković Institute, Zagreb, Croatia, as KBr pellets. Infrared spectra were obtained from 4000 to 450 cm^{-1} on a Perkin-Elmer Spectrum RXI FT-spectrometer.

Thermal measurements were performed in a Mettler-Toledo TGA/SDTA 850^e instrument at 10°C min^{-1} and nitrogen (purity above 99.996%) at a flow rate of 20 mL min^{-1} from 25°C to 600°C. The samples were placed in a standard aluminum crucible (40 μL).

The 1-D and 2-D homo- and heteronuclear ^1H, ^{13}C NMR spectra were recorded with a Bruker AV 600 spectrometer, operating at 600.133 MHz for ^1H and 150.917 MHz for ^{13}C. Samples were measured from DMSO-d_6 solutions at 25°C (298 K) in 5 mm NMR tubes. Chemical shifts (ppm) are referenced to TMS. Flame ionization detector (FID) resolutions in ^1H and ^{13}C NMR spectra were 0.29 and 0.54 Hz per point, respectively. The following measurement techniques were used: standard ^1H and ^{13}C gated proton decoupling, APT, COSY, HMQC, and HMBC; 2-D NMR spectra were measured in pulsed field gradient mode (*z*-gradient).

2.2. *Preparation of complexes*

2.2.1. General procedure. A warm water solution of ligand (25 mL) was added dropwise with stirring to an aqueous solution of metal salt (10 mL). The resultant clear solution was then left at room temperature allowing slow evaporation until X-ray quality crystals were formed. The crystals were filtered off, washed with small portions of cold water, and dried in air. The mercury compound, $[Hg(NO_3)(pia)_2](NO_3)$, was prepared as described [6c].

2.2.2. Preparation of (1). Used: $Ni(NO_3)_2 \cdot 6H_2O$ (0.29 g, 1 mmol) and picolinamide (0.24 g, 2 mmol). Yield: 83%. Elemental Anal. Calcd for $C_{12}H_{16}NiN_6O_{10}$ (**1**) (%): C, 31.1; H, 3.5; N, 18.2. Found: C, 31.3; H, 3.4; N, 18.3. FT-IR (cm^{-1}, KBr): 3394(s), 3181(s), 2758(w), 1670(vs), 1623(w), 1616(w), 1584(m), 1572(s), 1559(w), 1506(w), 1436(vs), 1384(vs), 1354(vs), 1301(m), 1180(w), 1159(w), 1119(m), 1091(w), 1052(w), 1026(m), 828(w), 783(m), 757(m), 667(m), 650(m), 619(m), 510(w).

2.2.3. Preparation of (2). Used: $Zn(NO_3)_2 \cdot 6H_2O$ (0.30 g, 1 mmol) and picolinamide (0.24 g, 2 mmol). Yield: 86%. Elemental Anal. Calcd for $C_{12}H_{16}ZnN_6O_{10}$ (**2**) (%): C, 30.7; H, 3.4; N, 17.9. Found: C, 30.6; H, 3.6; N, 17.8. FT-IR (KBr, cm^{-1}): 3394(s), 3248 (s), 3181(s), 2755(w), 1675(vs), 1636(w), 1612(w), 1586(m), 1572(s), 1507(w), 1433(vs), 1385(vs), 1358(vs), 1303(m), 1180(w), 1159(w), 1120(w), 1093(w), 1053(w), 1025(m), 983(w), 907(w), 828(w), 781(m), 756(m), 663(m), 648(m), 621(m), 508(w).

2.2.4. Preparation of (3). Used: $Cd(NO_3)_2 \cdot 4H_2O$ (0.31 g, 1 mmol) and picolinamide (0.24 g, 2 mmol). Yield: 74%. Elemental Anal. Calcd for $C_{12}H_{12}CdN_6O_8$ (**3**) (%): C, 30.0; H, 3.4; N, 17.5. Found: C, 30.1; H, 3.5; N, 18.3. FT-IR (KBr, cm^{-1}): 3398(s), 3337(s), 3183(s), 2754(w), 1671(vs), 1582(s), 1571(s), 1488(m), 1434(vs), 1383(vs), 1354(vs), 1300(s), 1227(m), 1178(w), 1158(m), 1118(m), 1090(m), 1051(w), 1021(m), 981(w), 906(w), 827(m), 783(s), 755(s), 664(s), 645(m), 620(m), 507(w).

2.3. *X-ray structural analysis*

General and crystal data, summary of intensity data collection, and structure refinement for **1**–**3** are given in table 1.

Data collections were carried out on an Oxford Diffraction Xcalibur four-circle kappa geometry single-crystal diffractometer with Sapphire 3 CCD detector, using graphite monochromated Mo-Kα ($\lambda = 0.71073$ Å) radiation, and applying the CrysAlis Software system [19] at 296 K. The crystal–detector distance was 50 mm. Data reduction, including absorption correction, was done by CrysAlis RED program [19].

The structures were solved by direct methods implemented in the SHELXS-97 program [20]. The coordinates and the anisotropic thermal parameters for all non-hydrogen atoms were refined by full-matrix least-squares methods based on F^2 using SHELXL-97 program [20]. The aromatic hydrogen atoms were generated geometrically using the riding model with the isotropic factor set at 1.2 U_{eq} of the parent atom. Hydrogen atoms on the carboxamide nitrogen were located in the difference Fourier map at the final stage of refinement and refined freely. Graphical work has been

Table 1. Crystal data and structure refinement for **1–3**.

Compounds	$[Ni(pia)_2(H_2O)_2](NO_3)_2$ (**1**)	$[Zn(pia)_2(H_2O)_2](NO_3)_2$ (**2**)	$[Cd(pia)_2(NO_3)_2]$ (**3**)
Empirical formula	$C_{12}H_{16}NiN_6O_{10}$	$C_{12}H_{16}ZnN_6O_{10}$	$C_{12}H_{12}CdN_6O_8$
Formula weight	463.0	469.70	480.69
Color and habit	Blue, prism	Colorless, block	Colorless, block
Crystal system	Monoclinic	Monoclinic	Monoclinic
Space group	$P2_1/c$	$P2_1/c$	$P2_1/c$
Unit cell dimensions (Å,°)			
a	6.9407(1)	6.9077(1)	7.1833(4)
b	11.0964(2)	11.2042(2)	14.7529(2)
c	13.0365(3)	13.0828(3)	16.7812(2)
β	113.891(2)	113.843(2)	108.242(1)
Volume (Å^3), Z	918.00(3), 2	926.13(3), 2	1689.00(4), 4
Calculated density (g cm^{-3})	1.675	1.684	1.890
Absorption coefficient (mm^{-1})	1.124	1.393	1.351
$F(000)$	476.0	480.0	952
Crystal size (mm^3)	0.20 × 0.22 × 0.58	0.35 × 0.44 × 0.60	0.34 × 0.45 × 0.58
θ range for the data collection (°)	3.88–30.00	3.86–30.00	4.27–27.00
h, k, l range	$-9 \le h \le 9$; $-15 \le k \le 15$; $-17 \le l \le 18$	$-9 \le h \le 9$; $-15 \le k \le 15$; $-18 \le l \le 18$	$-9 \le h \le 9$; $-15 \le k \le 15$; $-21 \le l \le 21$
Scan type	ω	ω	ω
No. reflections collected	13,885	13,071	26,559
No. independent reflections	2666	2676	3665
No. observed reflections [$I \ge 2\sigma(I)$]	2078	2030	3417
No. refined parameters	149	150	261
Goodness-of-fit on F^2, S[d]	1.054	1.092	1.110
R[a], wR[b] [$I \ge 2\sigma(I)$]	0.0269, 0.0668	0.0276, 0.0683	0.0237, 0.0581
R, wR (all data)	0.0269, 0.0732	0.0276, 0.0771	0.0237, 0.0592
g_1, g_2 in w[c]	0.0333, 0.2431	0.0329, 0.2547	0.0281, 1.1219
Max. and min. electron density (e Å^{-3})	0.293 and –0.299	0.257 and –0.275	0.543 and –0.410
Maximum Δ/σ	0.003	0.001	<0.001
Range of transmission factors min, max	0.57; 0.80	0.43; 0.61	0.52; 0.65
Extinction coefficient	none	0.040(3)	0.013(4)

[a] $R = \sum ||F_o| - |F_c|| / \sum |F_o|$.

[b] $wR = \left[\sum \left(F_o^2 - F_c^2\right)^2 / \sum w\left(F_o^2\right)^2\right]^{1/2}$.

[c] $w = 1/\left[\sigma^2\left(F_o^2\right) + (g_1 P)^2 + g_2 P\right]$ where $P = \left(F_o^2 + 2F_c^2\right)/3$.

[d] $S = \sum \left[w\left(F_o^2 - F_c^2\right)^2 / \left(N_{obs} - N_{param}\right)\right]^{1/2}$.

performed by ORTEP-3 *for Windows* [21] and Mercury 1.4.1 [22]. The thermal ellipsoids were drawn at the 30% probability level.

2.4. *Biological activity – the effect on phagocytosis*

The mean picolinamide concentration of 1.031 μM L^{-1} in normal plasma was recently determined [23]. Ingestion and microbicidal capacities of human peripheral blood monocytes and neutrophils after picolinamide or Zn complex addition in two concentrations (1 or 5 μM L^{-1}, water solution) were determined by combining techniques for determining ingestions and intracellular killing [24 and references therein]. At least 100 granulocytes and monocytes in every sample were recognized separately, and the number of ingested yeast cells was counted and expressed as ingestion index = number of ingested yeast cells/100 granulocytes or monocytes.

The microbicidal capacity was assessed by discriminating between dead and alive ingested yeast cells and expressed as a percentage of killing = number of dead yeasts/number of all ingested yeast cells × 100.

3. Results and discussion

3.1. *Structure descriptions*

All crystals were grown by slow evaporation of the reaction mixture under ambient conditions from two days to one week. Selected bond distances, angles, and details on hydrogen bond geometry are presented in table 2. The structures are shown in figures 1 and 2.

The structures of **1** and **2** are isomorphous and consist of centrosymmetrical $[M(pia)_2(H_2O)_2]^{2+}$ complex cations (pia = picolinamide) and nitrate anions (figure 1a). The metal(II) ions have a distorted octahedral coordination geometry made up of two *trans*-chelating picolinamides and two water molecules. The picolinamide is bound through *N*,*O*-donors forming five-membered chelate rings in one plane, while the fifth and sixth coordination sites are occupied by H_2O. Distortions in the coordination sphere are mainly imposed by the chelation of pia to metal(II).

Hydrogen bonding appears to be the main driving force for building the crystal structures of **1** and **2**. The carboxamide moities are not involved in either of two commonly observed supramolecular amide synthons, head-to-head R_2^2 (8) dimers or $C(4)$ chains (scheme 1, **I** and **II**) [25]. Instead, the neighboring molecules are linked through centrosymmetric R_4^4 (12) synthons into 1-D chains in the [1 –1 0] direction (scheme 1, **V**). The synthons involve the amide nitrogen atoms as double hydrogen bond donors and two nitrate oxygen atoms of each of nitrate as hydrogen bond acceptors, while the carboxamide oxygen atoms do not participate in synthon formation (figure 2b).

The structure of **3** consists of discrete neutral molecules in which the cadmium is coordinated by two chelating pia and two nitrates (figure 2a). One nitrate is tightly bound to cadmium through O6 with Cd–O bond length of 2.318(3) Å, comparable with the two $Cd–O_{amide}$ bond values. The next closest oxygen of the same nitrate, O7, is pushed a little bit out of the coordination sphere and placed over pyridine nitrogen N1, exhibiting longer Cd–O distance of 2.853(3) Å, that is still less than the sum of van der Waals radii (2.49 + 1.52 = 4.01 Å). The other nitrate is coordinated *via* two oxygen atoms having both Cd–O distances on the borderline of what can be considered as cadmium–oxygen bonds [Cd1–O3 2.540(4), Cd1–O4 2.609(3) Å]. Therefore, the coordination sphere of cadmium(II) could be best described as caped pentagonal bipyramid.

The crystal structure of **3** is stabilized by hydrogen bonding interactions (table 3). The amide group of one picolinamide participates in typical head-to-head hydrogen bonds, forming centrosymmetrical dimers described by the graph-set motif of R_2^2 (8) (scheme 1, **I**), while the amide of the other pia is involved in N–H···O hydrogen bond with two oxygen atoms of two symmetrically different nitrates from two adjacent molecules. Thus an extended 3-D hydrogen bonding framework is formed (figure 2b).

Table 2. Selected bond distances (Å) and angles (°) for **1–3**.

1			
Ni1–O1	2.041(1)	O1–Ni1–O1^{i}	180.00
Ni1–O2	2.064(2)	N1–Ni1–N1^{i}	180.00
Ni1–N1	2.052(1)	O1–Ni1–O2	89.48(6)
		O1–Ni1–N1	79.85(5)
		O1–Ni1–O2^{i}	90.52(6)
		O1–Ni1–N1^{i}	100.15(5)
		O2–Ni1–N1	88.32(6)
		O2–Ni1–N1^{i}	91.68(6)
2			
Zn1−O1	2.078(1)	O1—Zn1–O1^{i}	180.00
Zn1–O2	2.130(2)	N1–Zn1–N1^{i}	180.00
Zn1–N1	2.093(1)	O1–Zn1–O2	89.52(7)
		O1–Zn1–N1	78.71(5)
		O1–Zn1–O2^{i}	90.49(7)
		O1–Zn1–N1^{i}	101.29(5)
		O2–Zn1–N1	87.99(6)
		O2–Zn1–N1^{i}	92.01(6)
3			
Cd1–O1	2.396(2)	O1–Cd1–O2	94.14(5)
Cd1–O2	2.300(2)	O1–Cd1–O3	146.05(8)
Cd1–O3	2.543(4)	O1–Cd1–O4	166.16(7)
Cd1–O4	2.617(3)	O1–Cd1–O6	98.55(8)
Cd1–O6	2.321(3)	O1–Cd1–N1	70.17(6)
Cd1–O7	2.864(3)	O1–Cd1–N3	88.16(6)
Cd1–N1	2.322(2)	O2–Cd1–O3	102.29(9)
Cd1–N3	2.344(2)	O2–Cd1–O4	80.35(7)
		O2–Cd1–O6	151.48(8)
		O2–Cd1–N1	92.79(6)
		O2–Cd1–N3	71.00(6)
		O3–Cd1–O4	47.7(1)
		O3–Cd1–O6	80.8(1)
		O3–Cd1–N1	79.46(9)
		O3–Cd1–N3	125.18(9)
		O4–Cd1–O6	81.34(9)
		O4–Cd1–N1	122.49(8)
		O4–Cd1–N3	78.05(8)
		O6–Cd1–N1	115.52(8)
		O6–Cd1–N3	83.94(8)
		N1–Cd1–N3	152.21(7)

Symmetry code: ^{i} $-x+1, -y+1, -z+1$.

A survey on the Cambridge Structural Database (CSD) [5] revealed that octahedral complex cation, *trans*-$[M(pia)_2(H_2O)_2]^{2+}$, found in **1** and **2**, is present in the majority of picolinamide complexes reported, regardless of the anion, in halide complexes of cobalt, $[Co(pia)_2(H_2O)_2]Br_2$ [26a], nickel, $[Ni(pia)_2(H_2O)_2]Cl_2$ [26b] and $[Ni(pia)_2(H_2O)_2]Br_2$ [26c], copper, $[Cu(pia)_2(H_2O)_2]Cl_2$ [26d, e] and $[Cu(pia)_2(H_2O)_2]Br_2$ [26d], and zinc, $[Zn(pia)_2(H_2O)_2]I_2$ [26f]; squarate cobalt and copper complexes, $[Co(pia)_2(H_2O)_2](sq)_2$ [26g] and $[Cu(pia)_2(H_2O)_2](sq)_2$ [26h], respectively; acetate cobalt complex, $[Co(pia)_2(H_2O)_2](ac)_2$ [26i, j]; saccharine nickel complex, $[Ni(pia)_2(H_2O)_2](sac)_2$ [26k], and nitrate complex of cobalt, $[Co(pia)_2(H_2O)_2](NO_3)_2$ [26l]. In all these complexes the self-complementary amide hydrogen bonds (scheme 1, **I**) are not robust enough to accommodate usually disruptive counter ions and cocrystallized water molecules.

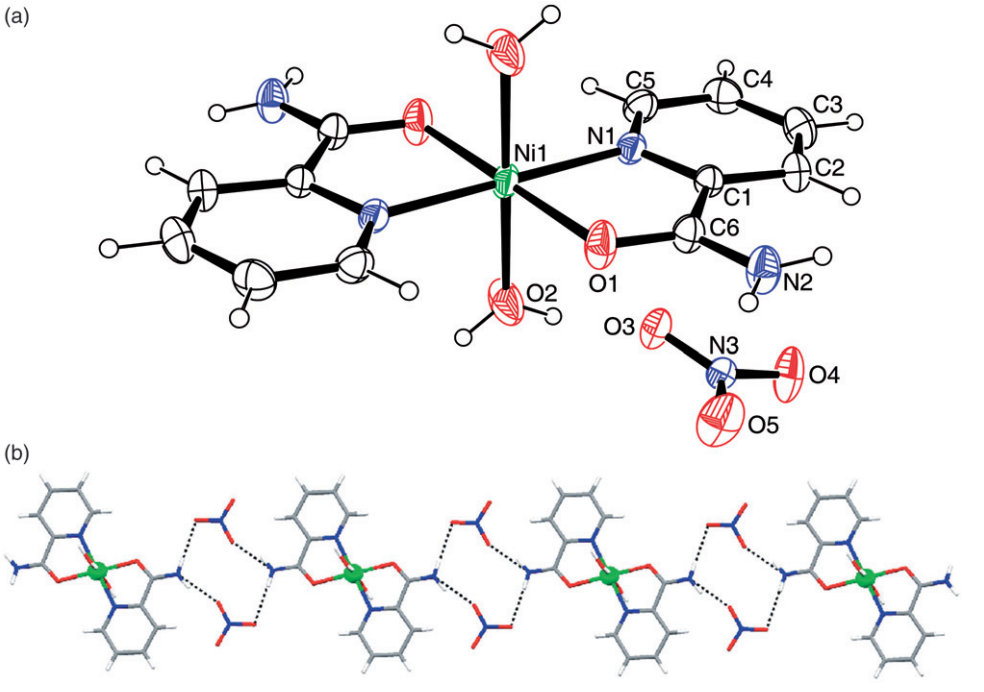

Figure 1. (a) ORTEP drawing of $[Ni(pia)_2(H_2O)_2](NO_3)_2$ (**1**) with atom numbering scheme of the asymmetric unit. Drawing for **2** corresponds to **1** without any significant difference. (b) Crystal packing of **1** and **2** viewed in the [1–1 0] direction with hydrogen bonds indicated by dotted lines. Only hydrogen bonds involving the carboxamide are represented (others, see table 3, are omitted for clarity).

However, several other motifs are found instead (scheme 1, **III–V**, **VII**), and these involve amide nitrogen atoms as double hydrogen bond donors.

Amide structures are frequently associated with an infinite ladder-like motif that is the result of a self-complementary R_2^2 (8) amide dimer accompanied by N–H···O interactions between the *anti* hydrogen of the $-NH_2$ group and the carbonyl oxygen of an adjacent amide moiety producing an R_4^2 (8) motif (scheme 2) [27]. The most frequently observed hydrogen bonding motif in the crystal structures of the picolinamide complexes, R_4^2 (8) tetramer, is similar to the one formed by two pairs of N–H···O interactions in the amide structures, only in the structures of picolinamide complexes, the amide oxygen is substituted by various hydrogen bonding acceptors, e.g., Cl, Br, I, N, S, from two additional adjacent molecules (scheme 1, **III**) forming supramolecular tetramers instead of dimers.

If the amide oxygen is replaced by certain oxoacid anions or carboxylic groups, different R_4^4 (12) motifs are formed (**IV–VI**) which might be regarded as extensions of the primary amide R_4^2 (8) synthon (**III**). Also, the substitution of the amide oxygen by squarate reveals extended R_4^4 (14) hydrogen-bonded motif (**VII**).

There are several other mononuclear octahedral bispicolinamide complexes, where anions are coordinated to metal(II). In some of these the amide groups participate in the R_4^2 (8) (**III**) ($[Zn(NCS)_2(pia)_2]$ [6a], $[Cd(HCOO)_2(pia)_2]$ [28]), while in others they participate in extended R_4^4 (12) synthon formations (**IV**), ($[Cu(ClO_4)_2(pia)_2]$

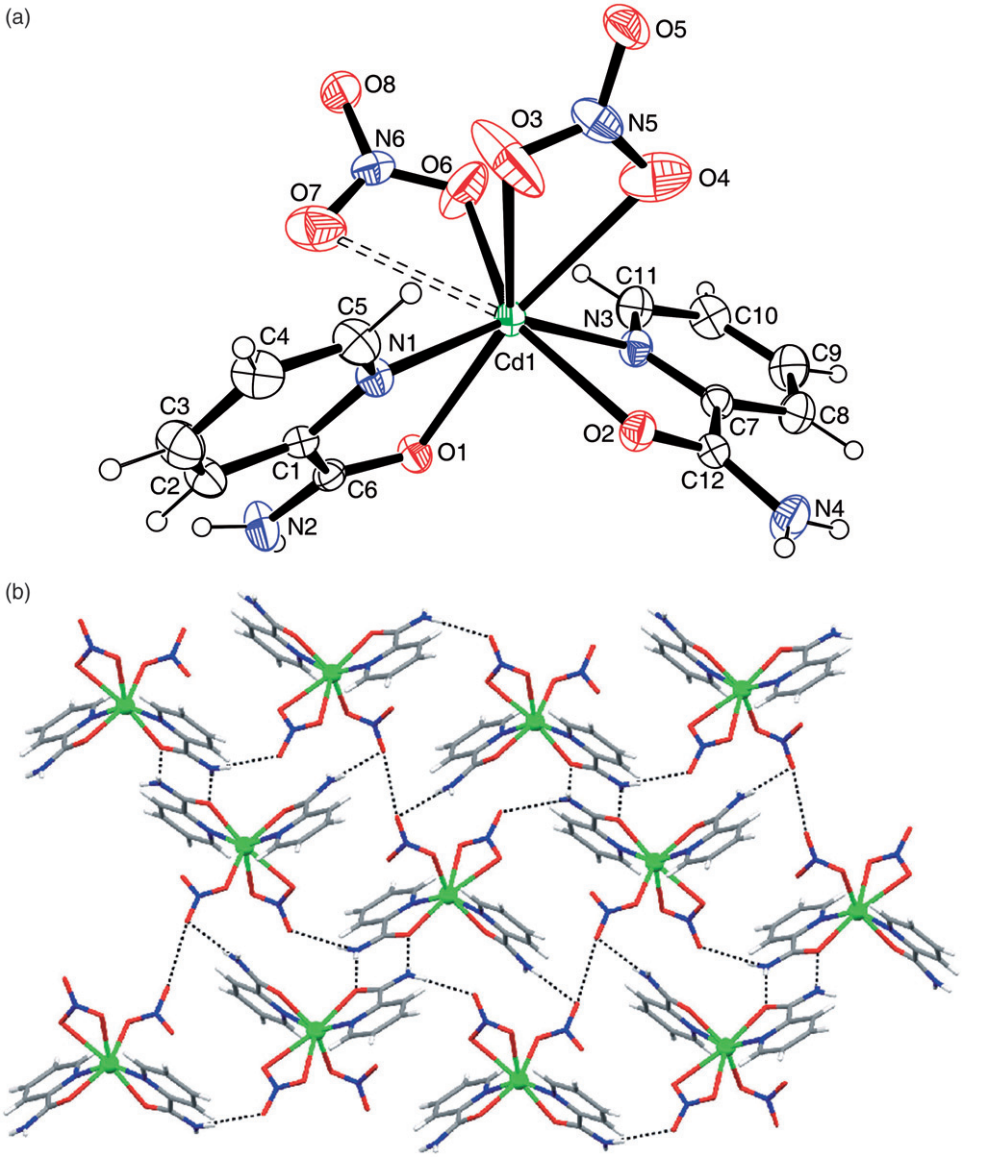

Figure 2. (a) ORTEP drawing of $[Cd(pia)_2(NO_3)_2]$ (**3**) with atom numbering scheme of the asymmetric unit. (b) Crystal packing of **3** viewed along the *b*-axis with hydrogen bonds indicated by dotted lines. Only hydrogen bonds involving the carboxamide are represented (others, see table 3, are omitted for clarity).

[29], $[Cu(HCOOCHCHCOO)_2(pia)_2]$ [30]). There are only three more octahedral bispicolinamide complexes, *cis*-$[Ni(N_3)_2(pia)_2]$ [6f], *trans*-$[Ni(N_3)_2(pia)_2]$ [6e], and $[Cu(NO_3)_2(pia)_2]$ [31], but in these the amide moieties are involved in more complicated hydrogen bond motifs.

The bispicolinamide complexes with metal(II) coordination number higher than six are rarely reported [5]. One is seven-coordinate mercury complex $[Hg(NO_3)(pia)_2](NO_3)$ [6c] which incorporates self-complementary amide bonding (**I**).

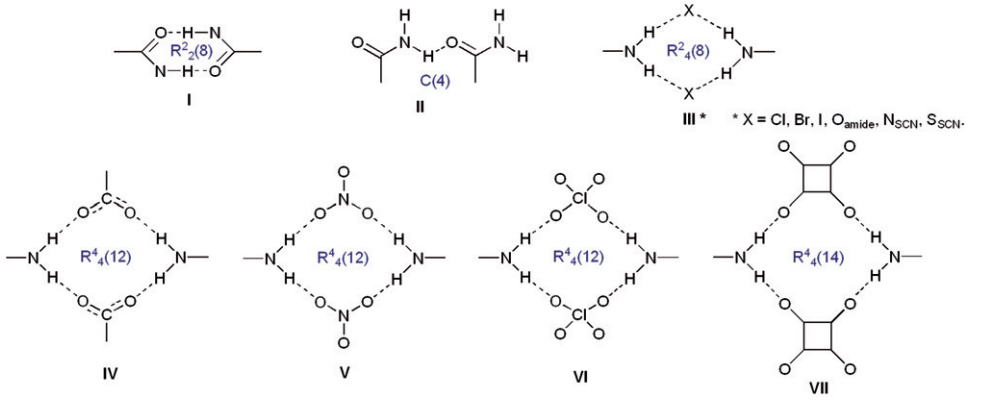

Scheme 1. The synthons involving the amide functionality of the picolinamide.

Table 3. Hydrogen bonds (Å and °) for **1–3**.

D–H···A	D–H	H···A	D···A	∠DHA	Symmetry code
1					
N2–H12N···O3	0.85(2)	2.08(3)	2.927(2)	176(2)	$x-1, y, z$
N2–H22N···O4	0.83(2)	2.16(2)	2.951(2)	159(2)	$-x+1, -y, -z+1$
O2–H8···O4	0.81(2)	2.36(2)	3.085(2)	150(3)	$-x+1, y+1/2, -z+1/2$
O2–H8···O5	0.81(2)	2.21(2)	2.955(2)	154(2)	$-x+1, y+1/2, -z+1/2$
O2–H8···N3	0.73(3)	2.62(3)	3.300(2)	154(3)	$x, y+1, z$
O2–H9···O3	0.84(2)	1.91(2)	2.742(2)	171(2)	x, y, z
C4–H4···O5	0.93	2.49	3.302(3)	147	$x+1, -y+1/2, z+1/2$
2					
N2–H12N···O3	0.91(3)	2.02(3)	2.926(2)	174(2)	$x-1, y, z$
N2–H22N···O4	0.84(2)	2.15(2)	2.945(2)	158(2)	$-x+1, -y, -z+1$
O2–H8···O4	0.82(2)	2.37(2)	3.110(3)	151(3)	$-x+1, y+1/2, -z+1/2$
O2–H8···O5	0.82(2)	2.18(2)	2.935(3)	153(2)	$-x+1, y+1/2, -z+1/2$
O2–H8···N3	0.73(3)	2.62(3)	3.300(2)	154(3)	$x, y+1, z$
O2–H9···O3	0.83(2)	1.93(2)	2.744(2)	169(2)	x, y, z
C4–H4···O5	0.93	2.50	3.299(3)	145	$x+1, -y+1/2, z+1/2$
3					
N2–H12N···O1	0.82(4)	2.15(3)	2.956(3)	170(3)	$-x+1, -y, z$
N2–H22N···O5	0.81(3)	2.20(3)	2.969(3)	161(3)	$x, -y+1/2, z-1/2$
N4–H14N···O5	0.83(4)	2.12(4)	2.931(4)	168(3)	$-x, y-1/2, -z+1/2$
N4–H24N···O8	0.82(4)	2.16(4)	2.959(3)	163(4)	$-x+1, y-1/2, -z+1/2$
C2–H2···O2	0.93	2.47	3.206(3)	136	$-x, -y, -z$
C3–H3···O4	0.93	2.55	3.269(4)	134	$x-1, -y+1/2, z-1/2$
C4–H4···O7	0.93	2.56	3.418(4)	154	$x-1, y, z$
C5–H5···O3	0.93	2.45	3.028(5)	120	x, y, z
C8–H8···O8	0.93	2.55	3.445(4)	161	$x+1, -y-1/2, z+1/2$
C11–H1···O6	0.93	2.55	3.126(4)	120	x, y, z

It is evident that the R_4^2 (8) motif dominates crystal structures of six-coordinate bispicolinamide complexes, while in others it may not be so. The outcome is in accord with our recent octahedral thiocyanate bispia complexes of Co, Ni, Cu, and Zn, where the R_4^2 (8) motif is energetically more favorable than the R_2^2 (8) one [32].

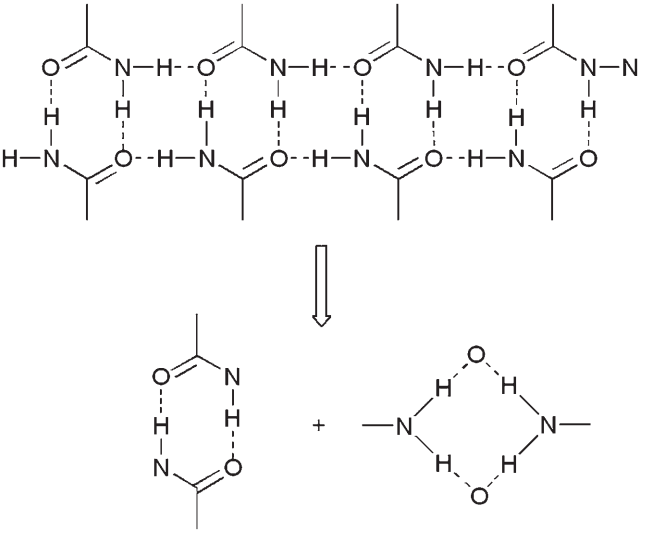

Scheme 2. The amide ladder-like motif decomposition.

3.2. *Spectroscopic properties*

3.2.1. IR spectra. The presence of a strong absorption in IR spectra of **1** and **2** at 1384 cm^{-1} and the absence of absorptions at 1540–1480 and 1290–1250 cm^{-1} suggest the presence of free nitrate in the complexes [33]. In the spectrum of **3** absorptions at 1488 and 1227 cm^{-1} are observed besides absorption at 1384 cm^{-1}, indicating the presence of coordinated nitrate. The noticeable positive shift of $\nu(C=O)_{am}$ in **1**–**3** points out the participation of both the carboxamide oxygen and aromatic nitrogen in coordination.

3.2.2. NMR spectra. The ^{1}H and ^{13}C NMR spectral data of free picolinamide and its Ni(II), Zn(II), Cd(II), and Hg(II) complexes are shown in table 4 and figure 3. Metal ion induced ^{1}H and ^{13}C NMR chemical shifts, i.e., complexation shifts, are defined as the difference of proton or carbon chemical shifts in the spectra of complex and free ligand. The enumeration of atoms, which is consistent with IUPAC nomenclature for this kind of compound, is displayed in scheme 3.

Proton chemical shifts for the free ligand measured in DMSO-d_6 [34] and DMF-d_7 [35] have been assigned previously. In ^{1}H NMR spectra of **2**–**4**, proton signals of picolinamide are shifted downfield with regard to signals in uncomplexed ligand, in the range 0.10–0.94 ppm. The greatest proton complexation shifts were observed in **4**, in accord with the electronic effect of mercury d-orbitals [36, 37].

In all complexes the complexation shifts ($\Delta\delta$) are smaller for pyridine ring protons than for the amide ones. For the latter the largest complexation shifts were 0.40–0.94 ppm. This is expected since the metal ion coordinating through the pyridine ring nitrogen reflects only slightly on the peripheral ring protons. However, the greatest complexation effect at amide protons is found in **4** which could be related to the

Table 4. ^{1}H and ^{13}C NMR chemical shifts (δ/ppm)[a] and metal induced chemical shifts ($\Delta\delta$/ppm),[b] H–H coupling constants ($^{n}J_{HH}$/Hz)[c] and C–H coupling constants ($^{n}J_{CH}$/Hz) of picolinamide and DMSO solution of **1**–**4**.

Molecule atom		Picolinamide	**1**[d]	**2**	**3**	**4**
H-3	Δ	8.18 (d)	8.00	8.30 (bs)	8.28 (bs)	8.53 (d)
	$^{3}J_{HH}$	7.80	–0.18	0.12	0.10	7.87
	$\Delta\delta$					0.35
H-4	δ	8.05 (t)	7.94 (bs)	8.20 (bs)	8.17 (t)	8.43 (t)
	$^{3}J_{HH}$	7.72	−0.11	0.15	7.81	7.72
	$\Delta\delta$				0.12	0.38
H-5	δ	7.65 (dd)	7.55 (bs)	7.79 (bs)	7.78 (dd)	8.08 (dd)
	$^{3}J_{HH}$	7.55; 4.77	−0.10	0.14	7.55; 4.49	7.33; 4.66
	$\Delta\delta$				0.13	0.43
H-6	δ	8.70 (d)	8.59 (b)	8.70 (b)	8.74 (d)	8.89 (d)
	$^{3}J_{HH}$	4.71	−0.11	0.00	4.77	4.78
	$\Delta\delta$				0.04	0.19
NH	Δ	7.84 (bs)	7.55 (bs)	8.50 (bs)	8.29 (bs)	8.78 (bs)
	$\Delta\delta$		−0.29	0.66	0.45	0.94
NH	Δ	8.30 (bs)	8.04 (bs)	8.86 (bs)	8.70 (bs)	9.18 (bs)
	$\Delta\delta$		−0.26	0.56	0.40	0.88
C=O	Δ	166.23 (s)	165.94 (s)	166.17 (s)	166.14 (s)	164.93 (s)
	$\Delta\delta$		−0.29	−0.06	−0.09	−1.3
C-2	Δ	150.31 (s)	150.22 (s)	147.10 (s)	148.24 (s)	143.83 (s)
	$\Delta\delta$		−0.09	−3.21	−2.07	−6.48
C-3	Δ	121.98 (d)	121.78 (d)	122.77 (d)	122.85 (d)	124.98 (d)
	J_{CH}	169.04	170.14	169.34	168.22	172.02
	$\Delta\delta$		−0.20	0.79	0.87	3.00
C-4	Δ	137.62 (d)	137.53 (d)	139.57 (d)	139.14 (d)	142.48 (d)
	J_{CH}	166.84	164.88	169.54	167.69	167.87
	$\Delta\delta$		−0.09	1.95	1.52	4.86
C-5	Δ	126.44 (d)	126.34 (d)	127.91 (d)	127.64 (d)	129.61 (d)
	J_{CH}	165.12	165.21	167.91	167.18	171.40
	$\Delta\delta$		−0.10	1.47	1.20	3.17
C-6	Δ	148.44 (d)	148.37 (d)	148.51 (d)	149.15 (d)	150.96 (d)
	J_{CH}	180.16	177.37	183.07	182.45	186.80
	$\Delta\delta$		−0.07	0.07	0.71	2.52

[a]Recorded in DMSO-d_6 solutions. Referred to TMS.
[b]Metal-induced chemical shifts ($\Delta\delta$/ppm) are obtained by subtracting the chemical shifts of parent compound (picolinamide) from the chemical shifts of metal complex.
Sign (+) denotes deshielding effect, while (–) denotes shielding effect of metal ion.
[c]n denotes the number of bonds between nuclei in spin–spin coupling; (s) singlet, (d) doublet, (t) triplet.
[d]Broadened (b)^{1}H NMR signals do not allow annotation of coupling constants.

mercury bonding to amide nitrogen, giving deshielding of amide protons in **4**. The amide protons, besides exerting electron redistribution upon complexation, are involved in hydrogen bonding which changes their chemical shifts. In **2**–**4** amide protons are more deshielded than in free pia, consistent with stronger hydrogen bonding in complexes than in ligand in solution. The stronger hydrogen bonding in **2** and **3** was determined by an X-ray analysis in solid state as well. Contrary to **2**–**4** in ^{1}H NMR spectra of **1**, a broadening and upfield shift of proton signals are observed from paramagnetic effect [38]. In addition to paramagnetic effects, the shielding of amide protons in **1** is also related to different hydrogen bonding in **1** than in **3** and **4**.

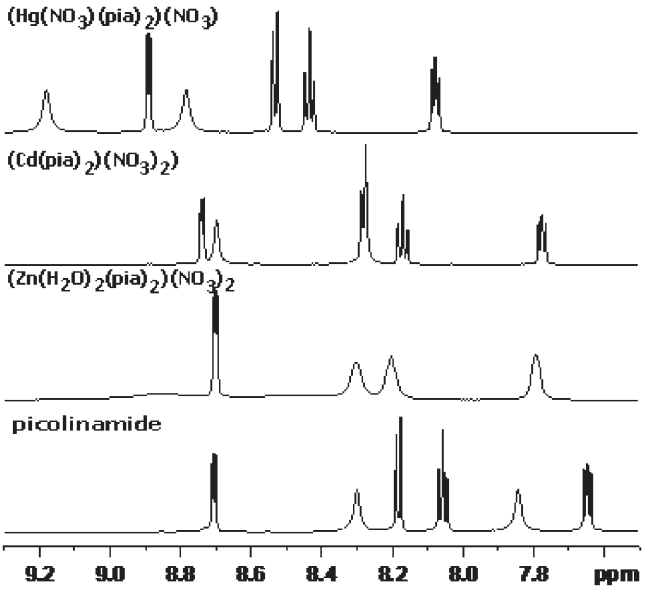

Figure 3. ^{1}H NMR spectra of DMSO-d_6 solutions of picolinamide and **2**–**4**.

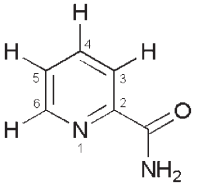

Scheme 3. Enumeration of the atoms in picolinamide.

This difference was observed in the solid state, where in **3** and **4** direct hydrogen bonding between molecules exists, while in **1** hydrogen bonding between two pairs of Ni(II) complexes takes place *via* two interfering NO_3 groups.

The ^{13}C NMR spectra of **1**–**4** displayed six signals consistent with picolinamide complexes, confirmed by X-ray data as well. The greatest changes of ^{13}C chemical shifts upon complexation were found for carbons in the mercury complex (**4**), while the lowest complexation effects were observed in nickel complex (**1**). In addition, in **1** all carbons are shielded with respect to parent picolinamide, while in **2**–**4** only C-2 and carboxamide carbons are shielded, while all others are deshielded. The paramagnetic effects in **1** are responsible for these differences. C-2 in **4** is the most shielded (−6.48 ppm) carbon in all complexes. As shown in table 4, complexation ^{13}C chemical shifts of carboxamide carbon observed in **2**, **3**, and **1** are −0.06, −0.09, and −0.29 ppm, respectively, while in **4** it is −1.30 ppm. Chemical shifts of the carboxamide carbons in **1**, **2**, and **3** are close to the carboxamide carbon chemical shift of the ligand, although in **1** additional paramagnetic effects increase this difference. These observations for carboxamide

carbons, together with the greater shielding at C-2 in **4**, can be related to the difference in metal–nitrogen complexation in **4** compared to **1**–**3**, which also reflects metal–nitrogen bond-length differences. As previously reported, the steric demand of nitrate oxygen atoms covalently bound to Hg(II) in **4** is probably responsible for these bond-length differences [6c]. The considerable difference in deshielding at C-3, C-4, C-5, and C-6 between **1**–**3** and **4** also corroborate different complexation patterns in these complexes.

On the basis of ^{1}H and ^{13}C NMR data from DMSO-d_6 solution, one can conclude that Ni(II), Zn(II), and Cd(II) complexation (**1**–**3**) occur through the pyridine ring nitrogen of the ligand, while Hg(II) complexation (**4**) takes place through the carboxamide of the ligand as well, forming an *N*,*O*-chelate.

3.3. *Thermal analysis*

The thermal behaviors of **1**–**3** were studied by TG/DTA thermal analysis from 25 to 600°C. Although isomorphous, **1** and **2** undergo different thermal decomposition. Their thermal gravimetric (TG) curves show similar thermal processes up to approximately 220°C. In that temperature interval, the compounds are stable to 130°C (**1**) and 100°C (**2**). At higher temperature dehydration occurs as a single mass-loss step, corresponding to 7.9% for **1** and 7.8% for **2** (Calcd 7.8 for **1** and 7.7% for **2**). The release of water was accompanied by an endothermic effect on the DTA curve at 171°C (**1**) and 117°C (**2**). The dehydrated products $[M(pia)_2](NO_3)_2$ (M = Ni, Zn) are further stable to 220°C. Above that temperature **1** rapidly loses 53.0% of its mass corresponding to the decomposition of two picolinamides (Calcd 52.8%), accompanied with a very sharp exothermic peak at 311°C. At 320–490°C decomposition proceeds in two poorly resolved steps followed by two exothermal events which correspond to the loss of two NO_2 molecules (found 20.2%; Calcd 19.9%, exo peak at 416°C) and one O_2 (found 7.4%; Calcd 6.9%, exo peak at 452°C). The final residue after 560°C (13.3%) corresponds to Ni (Calcd 12.7%).

Compound **2** decomposes in several consecutive, poorly resolved mass-loss steps above 220°C, which are followed by four small peaks in the DTA curve (endo at 282°C; exo at 342°C; very broad endo at 370–460°C; very broad exo at 460–570°C). The final residue of 14.1% obtained above 570°C corresponds to Zn (Calcd 13.9%).

Analysis of the TG and DTA curves of **3** shows that thermal decomposition consists of three major processes which are not well resolved in the TG curve. The first two very sharp peaks in the DTA curve (endothermic at 289°C and exothermic at 318°C) follow a mass loss of 49.3%. At 330–580°C two broad peaks in the DTA curve are recorded (the first endothermic and the second exothermic) that are accompanied with an overall mass loss of 27.8%. The final residue of 23.5% above 580°C corresponds to Cd (Calcd 23.3%).

3.4. *Biological activity – the effect on phagocytosis*

For both concentrations phagocytic functions – ingestion and intracellular killing – were determined of two samples of picolinamide, two samples of the Zn complex (**2**), and in a control physiological sample (table 5). Picolinamide and the Zn complex in granulocyte and monocyte cell suspension were well tolerated. Additionally, for both

Table 5. Neutrophil and monocyte ingestion and intracellular killing capacity without (control) and with picolinamide or the Zn complex (**2**) addition.

	Neutrophils				Monocytes			
	Ingestion index		Intracellular killing capacity (%)		Ingestion index		Intracellular killing capacity (%)	
	A	B	A	B	A	B	A	B
Control	2.83	2.99	10	12	1.05	0.87	45	55
Picolinamide	3.36	2.95	11	13	1.05	0.62	46	59
Picolinamide	3.44	3.10	8	7	1.08	1.02	50	47
$[Zn(H_2O)_2(pia)_2](NO_3)_2$ (**2**)	2.81	3.12	12	8	1.06	0.82	44	48
$[Zn(H_2O)_2(pia)_2](NO_3)_2$ (**2**)	2.74	3.11	7	6	1.51	1.11	35	39

Picolinamide and **2** were used in concentrations of $1\,\mu M\,L^{-1}$ (A) and $5\,\mu M\,L^{-1}$ (B).

concentrations there are indications of mild tendency of decline in the Zn complex samples for monocyte and neutrophil intracellular killing capacity in comparison with the control sample.

The data suggest that statistically significant difference in phagocytic function could be observed when using picolinamide or its Zn complex in various concentrations and larger sample sizes.

4. Conclusion

The picolinamide complexes of Ni(II) (**1**), Zn(II) (**2**), and Cd(II) (**3**) have been prepared, studied by spectral and thermal methods, and their structures are determined by SCXRD and solution ^1H and ^{13}C NMR spectra. The structure of the analogous picolinamide mercury(II) complex (**4**) in solution was determined. In crystalline state picolinamide is coordinated through the *N*,*O*-donor set, while in DMSO solutions it coordinates to Ni, Zn, and Cd through the pyridine ring, and through both atoms only to Hg(II). The neutral Cd complex (**3**) showed greater thermal stability than **1** and **2**. Above 570°C all three complexes were decomposed completely. In crystal structures of **1** and **2**, molecules are linked into supramolecular chains through R_4^4 (8) rings involving only the amide nitrogen atoms as double hydrogen bond donors, whereas in **3** the amide hydrogen R_2^2 (8) bonding persists. Mild tendency of decline for monocyte and neutrophil intracellular killing capacity is observed in $[Zn(H_2O)_2(pia)_2](NO_3)_2$.

Supplementary material

Crystallographic data for the structures reported in this article have been deposited with the Cambridge Crystallographic Data Centre as supplementary publication no. CCDC 816440 (**1**), 816441 (**2**), and 816442 (**3**). Copies of the data can be obtained free of charge at www.ccdc.cam.ac.uk/conts/retrieving.html [or from the Cambridge Crystallographic

Data Centre (CCDC), 12 Union Road, Cambridge CB2 1EZ, UK; Fax: +44(0)1223-336-033; or E-mail: deposit@ccdc.cam.ac.uk].

Acknowledgments

This research was supported by the Ministry of Science, Education, and Sports of the Republic of Croatia within the scientific projects under the titles ''Chemistry of metal complexes in reactions of biological importance and new materials'' (No. 119-1193079-1332), within the framework of the scientific program ''Ligands, complexes, proteins – synthesis and structure – properties relationship,'' and scientific projects under the titles ''NMR spectroscopy and modeling of bioactive molecules'' (No. 098-0982929-2917) and ''Circulating tumor cells in patients with solid tumors'' (No. 134-1342428-2427).

References

[1] W. Kaim, B. Schwederski. *Bioinorganic Chemistry: Inorganic Elements in the Chemistry of Life*, Wiley, Chichester (1994).
[2] T. Dudev, Y.-I. Lin, M. Dudev, C. Lim. *J. Am. Chem. Soc.*, **125**, 3168 (2003).
[3] H.S. Lee, G. Spraggon, P.G. Shultz, F. Wang. *J. Am. Chem. Soc.*, **131**, 2481 (2009).
[4] A. Siegel, H. Siegel. *Metal Ions in Biological Systems, Probing of Proteins by Metal Ions and Their Low-Molecular-Weight Complexes*, Vol. 38, Dekker, New York, Basel (2001).
[5] H.F. Allen. *Acta Crystallogr.*, **B58**, 380 (2002).
[6] (a) M. Đaković, Z. Popović, G. Giester, M. Rajić-Linarić. *Polyhedron*, **27**, 210 (2008); (b) M. Đaković, Z. Popović, G. Giester, M. Rajić-Linarić. *Polyhedron*, **27**, 465 (2008); (c) M. Đaković, Z. Popović. *Acta Crystallogr.*, **C63**, m557 (2007); (d) M. Đaković, Z. Jagličić, B. Kozlevčar, Z. Popović. *Polyhedron*, **29**, 1910 (2010); (e) M. Đaković, Z. Popović. *Acta Crystallogr.*, **C63**, m507 (2007); (f) M. Đaković, Z. Popović. *Acta Crystallogr.*, **E64**, m311 (2008); (g) M. Đaković, Z. Popović. *Acta Crystallogr.*, **C65**, m361 (2009); (h) M. Đaković, B.-M. Kukovec, Z. Popović. *Transition Met. Chem.*, **36**, 65 (2011); (i) M. Đaković, M. Došen, Z. Popović. *J. Chem. Crystallogr.*, **41**, 180 (2011).
[7] (a) R.A. Olsen, L. Liu, N. Ghaderi, A. Johns, M.E. Hatcher, L.J. Meuller. *J. Am. Chem. Soc.*, **125**, 10125 (2003); (b) T. Kabawa, T. Ogino, M. Mori, M. Awai. *Acta Pathol. Japan*, **42**, 469 (1992); (c) M.R. Horsman, D.W. Siemann, D.J. Chaplin, J. Overgaard. *Radiother. Oncol.*, **45**, 167 (1997).
[8] (a) K.-I. Sakai, T. Imakubo, M. Ichakawa, Y. Taniguchi. *J. Chem. Soc., Dalton Trans.*, 881 (2006); (b) E. Ueda, Y. Yoshikawa, Y. Ishino, H. Sakurai, Y. Kojima. *Chem. Pharm. Bull.*, **50**, 337 (2002).
[9] H. Below, H. Zöllner, H. Völzke, A. Kramer. *Int. J. Hyg. Environ. Health*, **211**, 186 (2008).
[10] Q. Wang, C. Feng, Y. Zhao, C. Hao. *Bioresource Technol.*, **100**, 2223 (2009).
[11] L.E. Braverman, X.M. He, S. Pino, M. Cross, B. Magnani, S.H. Lamm, M.B. Kruse, A. Engel, K.S. Crump, J.P. Gibbs. *J. Clin. Endocr. Metab.*, **90**, 700 (2005).
[12] A. Çelekli, M. Yavuzatmaca. *Bioresource Technol.*, **100**, 1847 (2009).
[13] B. Moulton, M.J. Zaworotko. *Chem. Rev.*, **101**, 1629 (2001).
[14] Y.Q. Zheng, J.L. Lin, Z.P. Kong. *Inorg. Chem.*, **43**, 2590 (2004).
[15] (a) C.B. Aakeröy, A.M. Beatty, D.S. Leinen, K.R. Lorimer. *Chem. Commun.*, 935 (2000); (b) C.B. Aakeröy, J. Desper, J. Valdés, J. Martínez. *CrystEngComm*, **6**, 413 (2004).
[16] T. Dorn, K.M. Fromm, C. Janiak. *Aust. J. Chem.*, **59**, 22 (2006).
[17] A.H. Shankar, A.S. Prasad. *Am. J. Clin. Nutr.*, **68**, 447S (1998).
[18] P. Krosgaard-Larsen, T. Lijefos, U. Madsen. *Textbook of Drug Design and Discovery*, 3rd Edn, Taylor and Francis, London (2004).
[19] Oxford Diffraction. *Xcalibur CCD System, CrysAlis (Version 171.31)*, Oxford Diffraction Ltd, Oxford (2004).
[20] G.M. Sheldrick. *Acta Crystallogr.*, **A64**, 112 (2008).
[21] L.J. Farrugia, ORTEP-3. *J. Appl. Crystallogr.*, **30**, 565 (1997).
[22] I.J. Bruno, J.C. Cole, P.R. Edgington, M.K. Kessler, C.F. Macrae, P. McCabe, J. Pearson, R. Taylor. *Acta Crystallogr.*, **B58**, 389 (2002).

[23] G.A. Smythe, A. Poljak, S. Bustamante, O. Braga, A. Maxwell, R. Grant, P. Sachdev. *Adv. Exp. Med. Biol.*, **527**, 705 (2003).
[24] J. Lukač, Z. Kusić, D. Kordić, M. Končar, A. Bolanča. *Breast Cancer Res. Treat.*, **29**, 279 (1994).
[25] (a) M.C. Etter. *Acc. Chem. Res.*, **23**, 120 (1990); (b) J. Bernstein, R.E. Davis, L. Shimoni, N.-L. Chang. *Angew. Chem., Int. Ed. Engl.*, **34**, 1555 (1995).
[26] (a) Q.-Y. Du, G.-Y. Zhang, Z.-Y. Hu, C.-H. Duan. *Xuaxue Yunjiu (Chin.) (Chem. Res.)*, **17**, 40 (2006); (b) A. Masuko, T. Nomura, Y. Saito. *Bull. Chem. Soc. Japan*, **40**, 511 (1967); (c) Q.-Y. Du, Y.-P. Li, L.-Y. Xin, M.-L. Han. *Z. Kristallogr. – New Cryst. Struct.*, **220**, 539 (2005); (d) L. Sieron, M. Bukowska–Strzyzewska. *Acta Crystallogr.*, **C53**, 296 (1997); (e) D.H. Brown, D.R. MacSween, M. Mercer, D.W.A. Sharp. *J. Chem. Soc. A*, 1574 (1971); (f) H. Paşuoglu, S. Guven, Z. Heren, O. Buyukgungor. *J. Mol. Struct.*, **794**, 270 (2006); (g) O.Z. Yesilel, H. Olmez, O.O. Yilan, H. Pasaouglu. O. Buyukgungor. *Z. Naturforsch*, **61b**, 1094 (2006); (h) I. Ucar, A. Bulut, O.Z. Yesilel, H. Olmez, O. Buyukgungor. *Acta Crystallogr.*, **E60**, m1945 (2004); (i) G.V. Tsintsadze, R.A. Kiguradze, A.N. Shnulin, I.R. Amiraslanov. *Gruz. Politekh. Inst.*, 5 (1980); (j) G.V. Tsintsadze, R.A. Kiguradze, A.N. Shnulin, Kh.S. Mamedov. *Zh. Strukt. Khim. (Russ.) (J. Struct. Chem.)*, **27**, 115 (1986); (k) H. Pasauoglu, F. Tezcan, O.Z. Yesilel, H. Olmez, H. Icbudak, O. Buyukgungor. *Acta Crystallogr.*, **C60**, m335 (2004); (l) B. Huang, L.-Y. Xin, Q.-Y. Du. *Xuaxue Shiji (Chin.) (Chem. Reagents)*, **29**, 132 (2007).
[27] C.B. Aakeröy, B.M.T. Scott, J. Desper. *New J. Chem.*, **31**, 2044 (2007).
[28] A.S. Batsanov, M.I. Matsaberidze, Y.T. Struchkov, G.V. Tsintsadze, T.I. Tsivtsivadze, L.V. Gverdtsiteli. *Koord. Khim. (Russ.) (Coord. Chem.)*, **12**, 1555 (1986).
[29] L. Sieron, M. Bukowska-Strzyzewska. *Acta Crystallogr.*, **C54**, 322 (1998).
[30] L. Sieron. *Acta Crystallogr.*, **E63**, m862 (2007).
[31] K.N. Lazarou, C.P. Raptopoulou, S.P. Perlepes, V. Psycharis. *Polyhedron*, **28**, 3185 (2009).
[32] M. Đaković, D. Vila-Viçosa, M.J. Calhordą, Z. Popović. *CrystEngComm*, **13**, 5863 (2011).
[33] Z. Popović, B. Korpar-Čolig, D. Matković-Čalogović, D. Vikić-Topić, M. Sikirica. *Main Group Chem.*, **1**, 373 (1996).
[34] W. Bruegel. *Z. Elektrochem. Ber. Bunsenges. Phys. Chem.*, **66**, 159 (1962).
[35] D.T. Hill, K. Burns, D.D. Titus, G.R. Girard, W.M. Reiff, L.M. Mascavage. *Inorg. Chim. Acta*, **346**, 1 (2003).
[36] B. Korpar-Čolig, Z. Popović, D. Matković-Čalogović, D. Vikić-Topić. *Organometallics*, **12**, 4708 (1993).
[37] Z. Popović, D. Matković-Čalogović, J. Hasić, D. Vikić-Topić. *Inorg. Chim. Acta*, **285**, 208 (1999).
[38] D.J. Harding, P. Harding, H. Adams, T. Tuntulani. *Inorg. Chim. Acta*, **360**, 3335 (2007).